Environmental Technology & Innovation 24 (2021) 101812

Contents lists available at ScienceDirect

Environmental Technology & Innovation

journal homepage: www.elsevier.com/locate/eti

Deposition of gum rosin microspheres on polypropylene microfibres used in face masks to enhance their hydrophobic behaviour

Cristina Pavon [a,*], Miguel Aldas [a,b], Emilio Rayón [a], Marina Patricia Arrieta [c,d], Juan López-Martínez [a]

[a] Instituto de Tecnología de Materiales, Universitat Politècnica de València (UPV), 03801 Alcoy-Alicante, Spain
[b] Departamento de Ciencia de Alimentos y Biotecnología, Facultad de Ingeniería Química y Agroindustria, Escuela Politécnica Nacional (EPN), Quito 170517, Ecuador
[c] Departamento de Ingeniería Química Industrial y del Medio Ambiente, Escuela Técnica Superior de Ingenieros Industriales, Universidad Politécnica de Madrid (ETSII-UPM), Calle José Gutiérrez Abascal 2, 28006 Madrid, Spain
[d] Grupo de Investigación: Polímeros, Caracterización y Aplicaciones (POLCA), 28006 Madrid, Spain

ARTICLE INFO

Article history:
Received 6 April 2021
Received in revised form 7 June 2021
Accepted 21 July 2021
Available online 23 July 2021

Keywords:
Gum rosin
Coating
Polypropylene
Electrospraying
Face mask
COVID-19

ABSTRACT

The present study aims to investigate the effects of gum rosin (GR) microspheres coating over the hydrophobicity of the outer layer of a polypropylene (PP) based surgical face mask. The gum rosin coating was deposited over the surface of the face mask outer layer by electrospraying technique. The deposition of GR microspheres was confirmed by field emission scanning electron microscopy (FESEM) and Fourier transform infrared spectroscopy (FTIR) analysis. The thermal analysis determined a cooperative effect between the microspheres and the mask fibre to increase the maximum degradation rate temperature and the onset degradation temperature. To follow the effect of the GR microspheres coating over the hydrophobicity of the surgical face mask, FESEM and wettability analyses were conducted before and after 3, 6, and 9 h of wearing time. In the FESEM image, it was seen that the microsphere was homogeneously distributed over the nonwoven fibre and its presence increases the roughness of the fibres due to the bulge of microspheres. The wettability measurements suggest that the microspheres coating helps to keep the original hydrophobicity of the outer layer of the surgical face mask even after 6 h of wearing time. Indeed, after 9 h of wearing time, the water contact angle (WCA) of the GR coated face mask is higher than the WCA of the surgical face mask without the coating at 3 h of wearing time. Therefore, the gun rosin microspheres coating improved the hydrophobicity of the surgical face mask which may allow improved protection and/or extended lifetime of use.

1. Introduction

The Coronavirus (CoV) is a large virus family composed of viruses that cause illness from the common cold to more severe diseases such as Middle East Respiratory Syndrome (MERS-CoV) and Severe Acute Respiratory Syndrome (SARS-CoV) (Abdi, 2020). SARS-CoV-2 is the causative agent of the ongoing pandemic of coronavirus disease 2019 (COVID-19) as

* Corresponding author.
E-mail address: crisppavonv@gmail.com (C. Pavon).

https://doi.org/10.1016/j.eti.2021.101812

it was determined by the World Health Organization (WHO), that within 12 months has infected more than 128 million individuals and caused more than 2 million deaths worldwide (Organisation, 2021).

Currently, there are no curative options available, and the WHO warns the efficacy of the vaccines depends on several factors and that they are not 100% effective (World Health Organization, 2020a,b). Therefore, among other measures, the massive use of mask in public places is highly recommended, and in some countries is mandatory to prevent the aerosol droplets spread of SARS-Cov-2 (Jefferson et al., 2009; Leung et al., 2020). There are different kinds of face masks available at the market guaranteeing different grades of protection mainly divided into surgical masks, respirators (FFP2 and FFP3 type by European standards or N95 and N99 by U.S. standards, respectively), and a basic cloth mask with two or more layers (Armentano et al., 2021; Krishnaswamy, 2020). Among all face masks, surgical face masks are the most widely used for common people, while they are also highly used by healthcare professionals. Surgical face masks have typically three polymeric layers mainly based on polypropylene (PP) as PP microfibres (Czigány and Ronkay, 2020). Nevertheless, the protective effect of the face masks can only be maintained when the surface of the mask is hydrophobic and dry (Li et al., 2006a). In fact, an increase in the mask surface moisture reduces the effectiveness in the protection of the mask and could become a culture medium for bacteria, which will allow bacterial contamination through the mask (Li et al., 2006b; Parlin et al., 2020). Thus, the possibility to extend the shelf life of face mask by increasing the surface hydrophobicity results very interesting, not only to increase the face mask effectiveness and reduce the chance to became a culture medium, but also to reduce the high amount of face masks used which represent a high amount of plastic waste which are currently directly discarded without any revalorization. The hydrophobicity of a surface is regulated by two factors, the surface roughness and the surface energy. Usually, a material with low surface energy poses a hydrophobic behaviour. The surface energy is determined by the chemical composition of the material (Gao et al., 2017). Therefore, modifying the surface roughness is possible to fabricate an hydrophobic surface (Kavitha Sri et al., 2020). To modify the surface roughness a variety of techniques can be used, for instance: chemical etching, plasma etching, solution immersion, electrodeposition, template deposition, spray coating, etc. (Kavitha Sri et al., 2020; Su et al., 2016). Several studies have proposed a solution to the hydrophobicity problem of the face masks, either by the addition of hydrophobic coatings with graphene (Zhong et al., 2020) or silica (Ray et al., 2020) or employing the incorporation of hydrophobic layers or membranes (El-Atab et al., 2020). Additionally, coatings of silver nanoparticles have been studied to provide an antimicrobial effect (Li et al., 2006a). However, the used methods require multistep manipulation, special equipment and post-treatment of the materials. Therefore, it is desirable to study a simple but versatile method to enhance the microstructure of a surface such as electrospraying or electrospinning, which are electrohydrodynamic process.

The electrohydrodynamic process are an easy and currently scalable technique that allow the deposition of many substances on various types of surfaces such as plastics, metals, woven, and non-woven materials (Fabra et al., 2016; Khan et al., 2017; Lasprilla-Botero et al., 2018). It is one of the most effective methods when low amounts of material are required to be deposited. It is a simple and flexible method and does not require additional treatments (i.e.: thermal treatments) to the final product. One disadvantages of the electrohydrodynamic process use to be its low productivity (usually with a processing throughput of a few millilitres per hour per single emitter). Nevertheless, nowadays electrohydrodynamic process is used at industrial scale level for the production of commercial products and recognized as cost-effective for materials commercial production (Arrieta et al., 2020), including face masks. Additionally, different shapes of microparticles can be obtained by electrospraying or electospinning techniques, which provides allotropic advantages (Alehosseini et al., 2018; Anu Bhushani and Anandharamakrishnan, 2014) and can easily modify the surface properties of the treated materials (Arrieta et al., 2019; Kavitha Sri et al., 2020). Moreover, the obtained particles fibre or spheres range between 5 μm to 0.05 μm, which is enough to create necessary roughness for attaining the non-wetting surface property (Kavitha Sri et al., 2020; Pavon et al., 2021).

As mentioned before, the other mechanism used to change the hydrophobicity of a surface is the use of a material with low surface energy and thus hydrophobic properties as a coating. Gum rosin is a natural hydrophobic compound that has intrinsic acidity and rigidity (Mahendra, 2019; Sharma and Singh, 2018; Yao and Tang, 2013). Gum rosin is the non-volatile fraction of pine resin and is mainly composed of abietic- and pimaric-type resin acids with hydrophobic hydrophenanthrene rings (Termentzi et al., 2011; Yadav et al., 2016). In blends with biodegradable plastics, gum rosin has shown its ability to increase the hydrophobicity of the final material (Pavon et al., 2020b,a). Additionally, the intrinsic hydrophobicity of gum rosin can be improved when it is produced in micro-and nano-sizes by a simple electrohydrodynamic process (Baek et al., 2011; Pavon et al., 2021). Gum rosin is biodegradable and biocompatible material (Satturwar et al., 2003). Moreover, coniferous gum rosin has been proven to have antimicrobial activity (Termentzi et al., 2011) against a wide range of microbes in the European Pharmacopoeia (EP) challenge test, including gram-positive (*S. aureus,* MRSA, *B. subtilis*) and gram-negative bacteria (*E. coli, P. aeruginosa*) as well as against yeasts, like *C. albicans* (Sipponen and Laitinen, 2011). Unmodified gum rosin does not produce adverse health effects or irritation of the respiratory tract after inhalation (as classified using animal models) (Santa Cruz Biotechnology Inc., 2009). It should be taken into account that gum rosin is classified as a skin sensitizer within the European Union (EC) (Karlberg, 2000). Due to the fact that it may cause skins sensitization if main abietadienes acids of rosin are oxidized (Karlberg, 2000; Karlberg et al., 1995) people with known contact allergy to rosin should avoid its contact (Sipponen and Laitinen, 2011).

The present work aims to enhance the surgical face mask hydrophobicity by a simple and scalable method taking advantages of two know mechanisms to increase surface hydrophobicuty, (1) the increase of the surface roughness and (2) the use of an intrinsic hydrophobic material. For this purpose, gum rosin was selected as hydrophobic material and it was

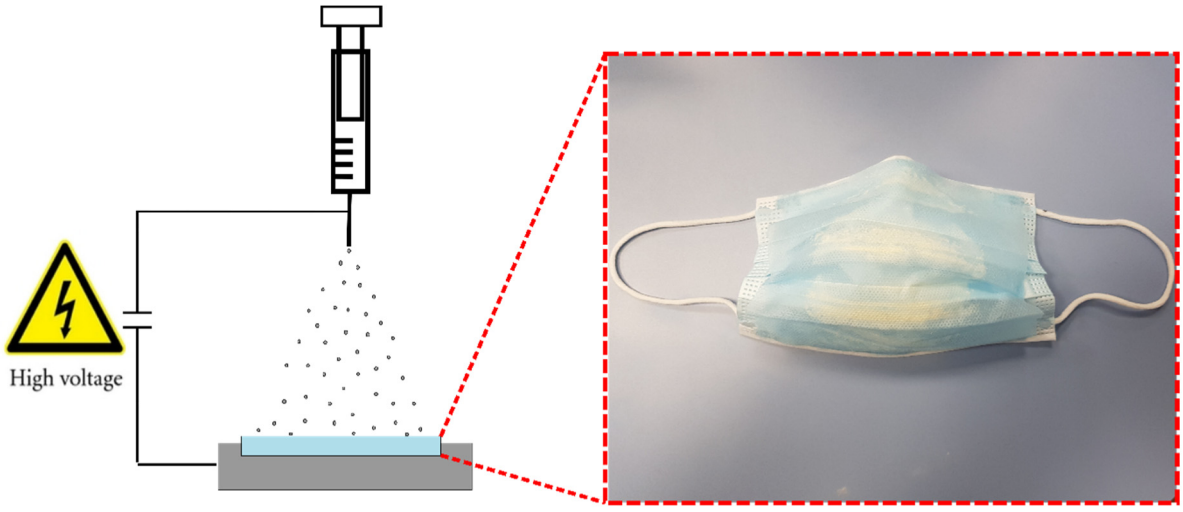

Fig. 1. Schematical representation of the electrospraying process and image of the outer layer of surgical mask with the microspheres coating.

incorporated by means of a simple electrostatic spraying process to obtain GR microspheres. Thus, GR was electrosprayed over the outer surface of a PP-based surgical face mask. Then, the mask has been characterized through thermal analyses and Fourier transform infrared spectroscopy confirming the deposition of GR into the face mask. Additionally, the microstructure and wettability of the mask have been analysed for 3, 6, and 9 h of wearing time demonstrating how the addition of GR microspheres improve the surface hydrophobicity of the surgical mask during wearing time extending their service life.

2. Materials and methods

2.1. Materials

Gum rosin (GR) commercial-grade was supplied Sigma-Aldrich (Mostoles, Spain) and was used for electrospray the outer layer of a surgical face mask. GR is characterized by a softening point of 76 °C, an acid number of 167, and a value of 4+ on the Gardner scale. Chloroform (CF) was used as a solvent and it was supplied by Panreac (Barcelona, Spain) with a density > 1.48 g/cm^3 at 20 °C and 99.8% purity. The mask used in the study was a commercial three-layer surgical face mask approved by the UNE 0064 standard.

2.2. Gum rosin electrospraying deposition onto surgical face mask

A 45 w/v gum rosin solution was prepared using chloroform as solvent. Chloroform was selected as solvent since it has been considered as an effective solvent for electrodynamic process due to its high evaporation rate (boiling point 60 °C) that allows effective solvent evaporation during processing (Arrieta et al., 2019). The electrospraying of gum rosin solution using chloroform as solvent- was optimized in a previous work (Pavon et al., 2021). In brief, the solution was kept under constant stirring at room temperature for 24 h. The solution was fed into a Higher Pressure Programmable Single Syringe Pump NE-1010 (Shropshire, United Kingdom). The pump was connected to a metallic needle with an internal diameter of 0.4 mm through polytetrafluoroethylene (PTFE) tubes. the needle tip was connected to a high voltage 0–30 kV power supply Genvolt 7xx30 series (Shropshire, United Kingdom). The electrospraying process was carried out in the outer layer of the surgical face masks as it is the layer in charge to repel water (Tcharkhtchi et al., 2021). To deposit the coating of gum rosin microspheres over a surgical face mask, the mask was set over the collector plate of the electrospraying system with its outer layer facing up. The working distance between tip to the substrate was of 15 cm. The microspheres were electrosprayed for 4 h with an applied voltage of 10 kV (positive and negative voltages = 5 kV and −5 kV, respectively) with a flow rate of 5 μL/min. The final aspect of the surgical mask after the electrospraying process is depicted in Fig. 1.

After the electrospraying process, the surgical face masks were vacuum dried in a desiccator for 1 week to remove any residual solvent. The wearing test were performed by three volunteers from our laboratory. Each volunteer wears a surgical face mask with (M-eGR) and without (M) gum rosin microspheres during 3, 6, and 9 h. In total 18 face mask were evaluated. During this time the volunteers were performing the daily activities of the work laboratory for instance: preparation and characterization of materials, manipulations of materials, analysis of results, writing of informs, etc. After these wearing times, the outer layer of the mask was characterized to get information on the behaviour of the face masks due to the addition of gum rosin microspheres coating.

2.3. Surgical face mask characterization

2.3.1. Thermal characterization

Differential scanning calorimetry (DSC) was conducted in a DSC 821 de Mettler-Toledo Inc. (Schwerzenbach, Switzerland). The thermal cycle consists of a first scan from 25 °C to 220 °C, followed by a cooling cycle from 220 °C to 25 °C, and a second heating scan from 25 °C to 400 °C. The heating and cooling rate in all cycles were 10 °C/min and the tests were performed in a nitrogen atmosphere with a flow rate of 30 mL/min. The second heating curve is reported.

Thermogravimetric analysis (TGA) was conducted in a TGA PT1000 from Linseis (Selb, Germany). Samples were heated from 30 to 700 °C at a heating rate of 10 °C/min in a nitrogen atmosphere with a flow rate of 30 mL/min. The onset ($T_{5\%}$) and endset ($T_{90\%}$) degradation temperature were determined at 5% and 90% of its initial mass loss, respectively. Additionally, the maximum degradation rate temperature (T_{max}) was determined at the minimum (peak) of the first derivative of the TGA curve (DTG)

2.3.2. Attenuated total reflectance-Fourier transform infrared spectroscopy characterization

Attenuated total reflectance-Fourier transform infrared spectroscopy (FTIR-ATR) was performed in a Perkin Elmer Spectrum BX (FTIR system) coupled with an ATR Pike MIRacle ™ (Beaconsfield, United Kingdom). The analyses were performed in the range of 4000–700 cm^{-1} with a resolution of 16 cm^{-1} and 20 scans.

2.3.3. Morphological characterization

The morphology of the outer layer of the face mask was studied by optical transmission microscopy in a Nikon Eclipse LV100 optical microscope under transmitted light. A size distribution of the gap between the fibres was elaborated in the outer layer of the face masks using the software ImageJ in the microscopic images.

2.4. Microstructure and wettability of the electrosprayed masks respect the wearing time

The effect of the GR microspheres coating over the microstructure and hydrophobicity of the face mask was analysed at 0, 3, 6, and 9 h of use by Field emission scanning electron microscopy (FESEM) to see the changes in the microstructure as well as by wettability measurements to measure the water contact angle of the face mask surface.

The FESEM analysis was performed using a Zeiss Ultra 55 microscope, operating at 1 kV. Before the analysis, the samples were mounted on aluminium stubs using double-sided adhesive tape and coated with a gold-palladium alloy layer for improved conduction with a Sputter Mod Coater Emitech SC7620, Quorum Technologies (East Sussex, UK).

The surface wettability of the outer layer of the surgical face mask was determined by water contact angle (WCA) by the sessile drop method. Water contact angle was measured using an optical goniometer EasyDrop-FM140 from Kruss Equipments (Hamburg, Germany) at room temperature (25 °C). Six water droplets ($\approx$1.5μL) were randomly deposited on the sample surface with a precision syringe and the average value of eight measurements for each droplet were used to create one data point. The significant differences in water contact angle were statistically assessed at 95% confidence level according to Tukey's test using a one-way analysis of variance (ANOVA) using OriginPro2015 software.

3. Results and discussion

3.1. Surgical face mask characterization

The DSC thermal curves of a surgical face mask with and without gum rosin (GR) microspheres, along with the thermal curve of neat gum rosin are plotted in Fig. 2. It is seen that the outer layer of the surgical face mask is fabricated with a single polymer, which appears to be polypropylene due to its glass transition temperature (T_g) and its melting temperature (T_m) (Calhoun, 2016; Grebowicz et al., 1984).

Furthermore, the coating of gum rosin microspheres caused no significant changes in the DSC curve of the surgical face mask, which could be attributed to: (i) the small amount of GR present in the coating among with the low sensibility of the DSC analyses and (ii) the amorphous nature of GR (Gaillard et al., 2011), which is confirmed by the absence of the melting peak in its respective DSC curve. However, it is observed that the GR microspheres coating protects the microfibres of the mask from thermal degradation. In the surgical face mask, the thermal degradation starts at 360 °C. Nevertheless, the degradation is not detected in the mask with the microspheres coating due to the GR microspheres coating.

The thermal stability of surgical face mask with and without gum rosin microspheres was confirmed by thermogravimetric analysis. The results are presented in terms of thermogravimetric curves in Fig. 3a and through its first derivative which are plotted in Fig. 3b. Regarding the surgical face mask, the typical complete weight loss in a single degradation step of PP is observed (Samper et al., 2018). Moreover, it is observed that the onset degradation temperature ($T_{5\%}$) is located at 283 °C, the endset degradation temperature ($T_{90\%}$) is found at 402 °C and the maximum rate degradation temperature (T_{max}) is placed at 389 °C. Meanwhile, neat GR presents lower temperatures than the M sample, since $T_{5\%}$ is 228 °C and $T_{max\%}$ is 314 °C. However, $T_{90\%}$ of gum rosin is 150 °C higher than the M sample, which explains the improvement in the thermal degradation of the surgical face mask observed in the DSC curve due to the GR microspheres coating. $T_{5\%}$ of M-eGR (242 °C) confirms the deposition of GR microspheres in the outer layer, as the decomposition temperature is

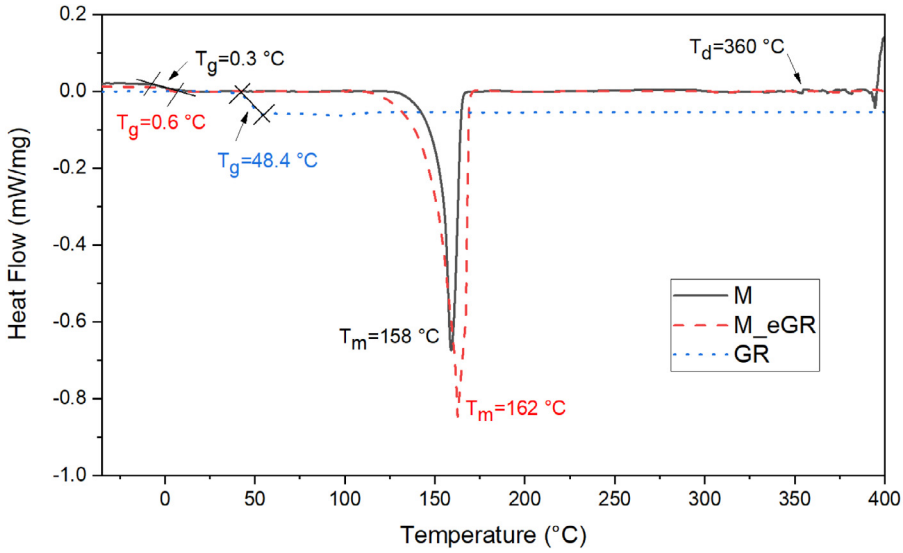

Fig. 2. (a) DSC curves of the outer layer of surgical mask with and without gum rosin microspheres coating and neat gum rosin.

closer to that of GR. Nonetheless, a successful deposition of GR microspheres in the outer layer of the surgical face mask is confirmed due to the increase in both $T_{90\%}$ and $T_{max\%}$ (421 °C and 405 °C respectively) which suggest a synergistic interaction between GR microspheres and polypropylene microfibres.

FTIR spectra of the outer layer of surgical mask with and without gum rosin microspheres coating and neat gum rosin are depicted in Fig. 4. The M spectrum is the typical spectra of polypropylene, confirming that this polymer is the sole component of the outer layer. The band corresponding to C–C stretching are located at 808, 973, and 996 cm^{-1}, the C-H rocking and wagging bands are found at 840 and 1162 cm^{-1} respectively. At 840, 996, and 1162 cm^{-1} the rocking modes of CH_3 are observed, in 1373 and 1456 cm^{-1} the symmetrical bending of CH_3 is seen as high-intensity bands in the spectra. The peaks at 2870 cm^{-1} and 2950 cm^{-1} at the high intensity and strong band indicate the stretching and asymmetrical stretching of the CH_3 group, while, the band at 2918 cm^{-1} correspond to the asymmetrical stretching of the CH_2 group (Fang et al., 2012). The obtained GR spectrum is the common spectra of gum rosin (Aldas et al., 2020), the high-intensity peak at 2944 cm^{-1} and the small peak at 2872 cm^{-1} indicate the strong stretching vibration modes of the CH_3 and CH_2 groups in hydrocarbon structures with three rings typical of diterpenes (Favvas et al., 2015). The band of C=O bonding is seen at 1694 cm^{-1} (Cabaret et al., 2018; Correa et al., 2018). The characteristic band to identify gum rosin is located at 2652 and 2536 cm^{-1} as a broad double structured band with peaks at. This band corresponds to the overtone stretching of the carboxyl group (Favvas et al., 2015). Moreover, in the fingerprint section between 1500 and 600 cm^{-1}, the absorption bands found between 1200 cm^{-1} and 800 cm^{-1} are characteristic of diterpenic resins (Azémard et al., 2014).

The M-eGR spectrum confirms the deposition of gum rosin microspheres over the surgical face mask surface. It presents features of gum rosin spectra as the C=O bonding, the characteristic bands of GR, and the fingerprint region. However, from 3500 to 3000 cm^{-1} the spectrum is more similar to polypropylene. This zone is related to the environmental moisture absorption, which indicates that the gum rosin microspheres are less prone to absorb moisture from the environmental humidity (Favvas et al., 2015).

3.2. Morphological characterization

In Fig. 5 the optical transmission microscopic images, among their respective sizes distribution of the gap between the fibres, of the outer layer of surgical face mask with and without GR microspheres coating is shown. In the surgical face mask without GR microspheres coating (Fig. 5a), it is seen that the non-woven PP microfibres form a mesh highly crisscross with high free space that allow airflow. The gap between the fibres' range between 25 and 75 μm. In the surgical face mask with GR microspheres coating (Fig. 5b). It is seen that the changes in the morphology of the face mask due to the addition of gum rosin microspheres are negligible. Besides the gap between the fibres' range stays the same. Therefore, it seems that the coating of gum rosin microspheres did not compromise the breathability of the surgical face masks (Ray et al., 2020), at least from an structural point of view and in good accordance with the perception of volunteers, who did not notice any breathability difference between both face masks.

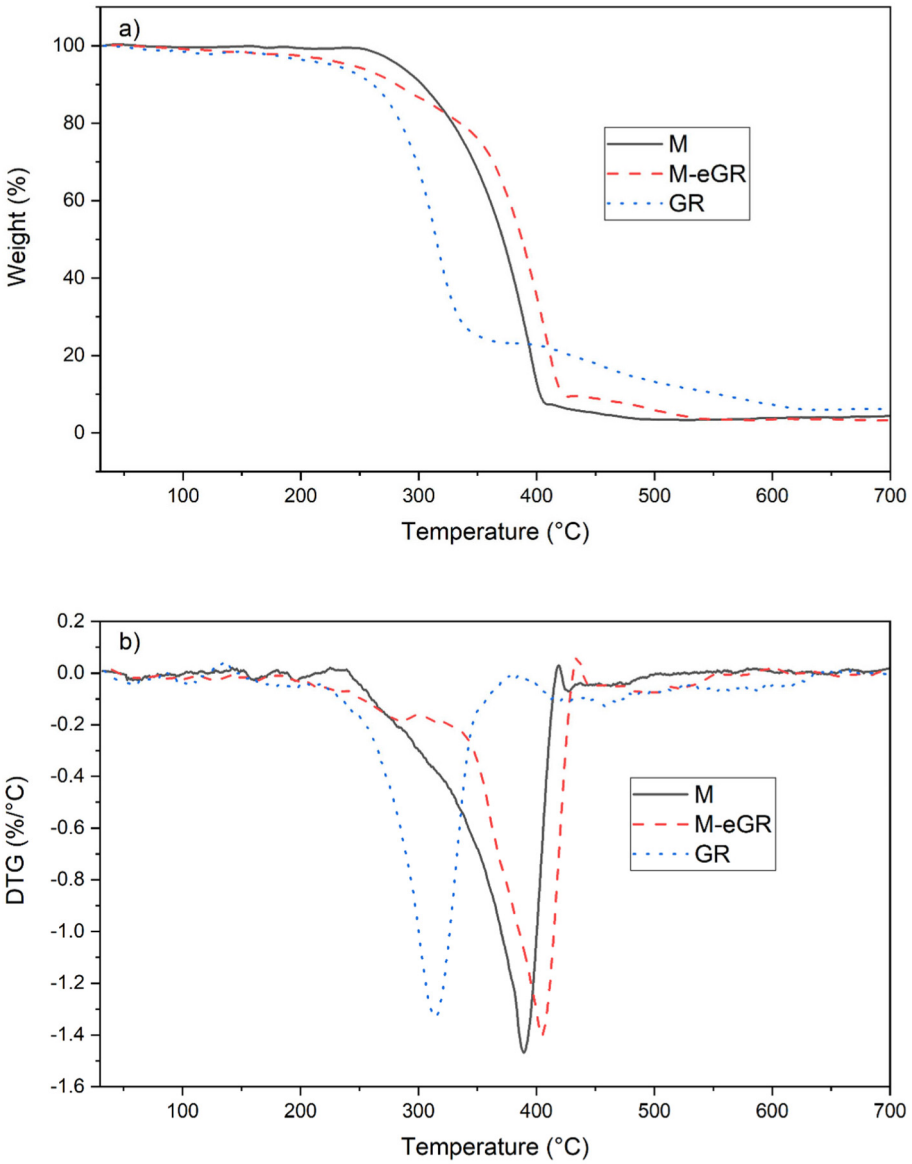

Fig. 3. (a) TGA and (b) DTG curves of the outer layer of surgical mask with and without gum rosin microspheres coating, and neat gum rosin.

3.3. Microstructure and wettability of the electrosprayed masks respect the wearing time

The FESEM images of test samples of surgical face masks are shown in Fig. 6. The neat surface of a surgical face mask (Fig. 6a) shows that the polypropylene microfibres are randomly placed and that the structure forms a non-woven mesh. No significant changes were detected by FESEM in the microstructure of the neat face mask due to the time of use of the mask (Fig. 6a, Fig. 6c, Fig. 6e, and Fig. 6g). On the other hand, Fig. 6b (0 h of wearing time) shows that microspheres were successfully deposited over the surface of the surgical face mask. It is observed that the gum rosin microspheres have highly adhered to the non-woven fibres that make up the mask and that its presence increases the roughness of the fibres due to the bulge of microspheres. Besides, a homogeneous microsphere distribution upon the non-woven fibres can be seen. After 3 wearing hours (Fig. 6d), the microspheres are still well adhered to the fibres with no significant changes in the microstructure. However, after 6 wearing hours (Fig. 6f), even when the density of microspheres is still high, the microspheres begin to detach from mask fibres, letting some part of the fibre uncovered. Finally, after 9 h of wearing time (Fig. 6h), it is seen that most of the microspheres have been removed from the mask. Nevertheless, it should be highlighted that the surface is not completely free from microspheres and the microstructure respect the mask without the coating is still different (Fig. 6g).

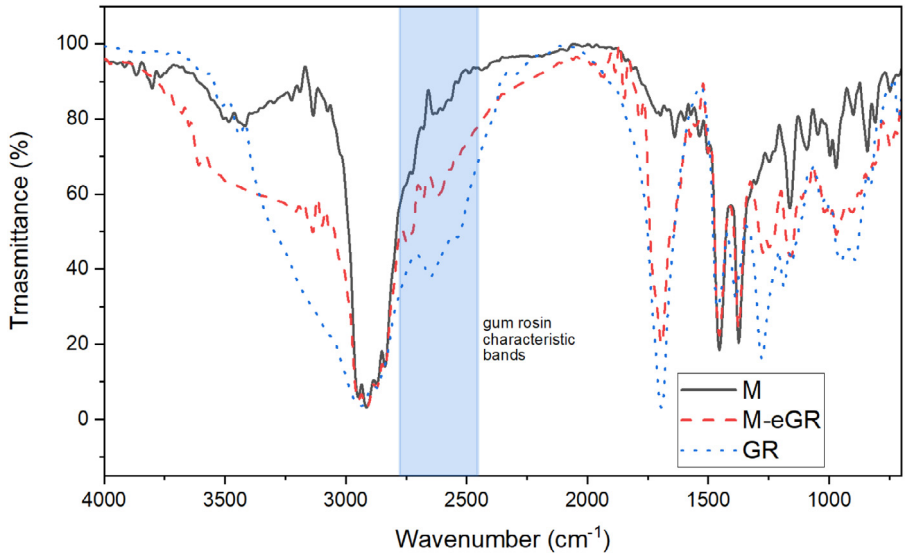

Fig. 4. Fourier-transform infrared spectroscopy (FTIR) spectra of the outer layer of surgical face mask with and without gum rosin microspheres and neat gum rosin.

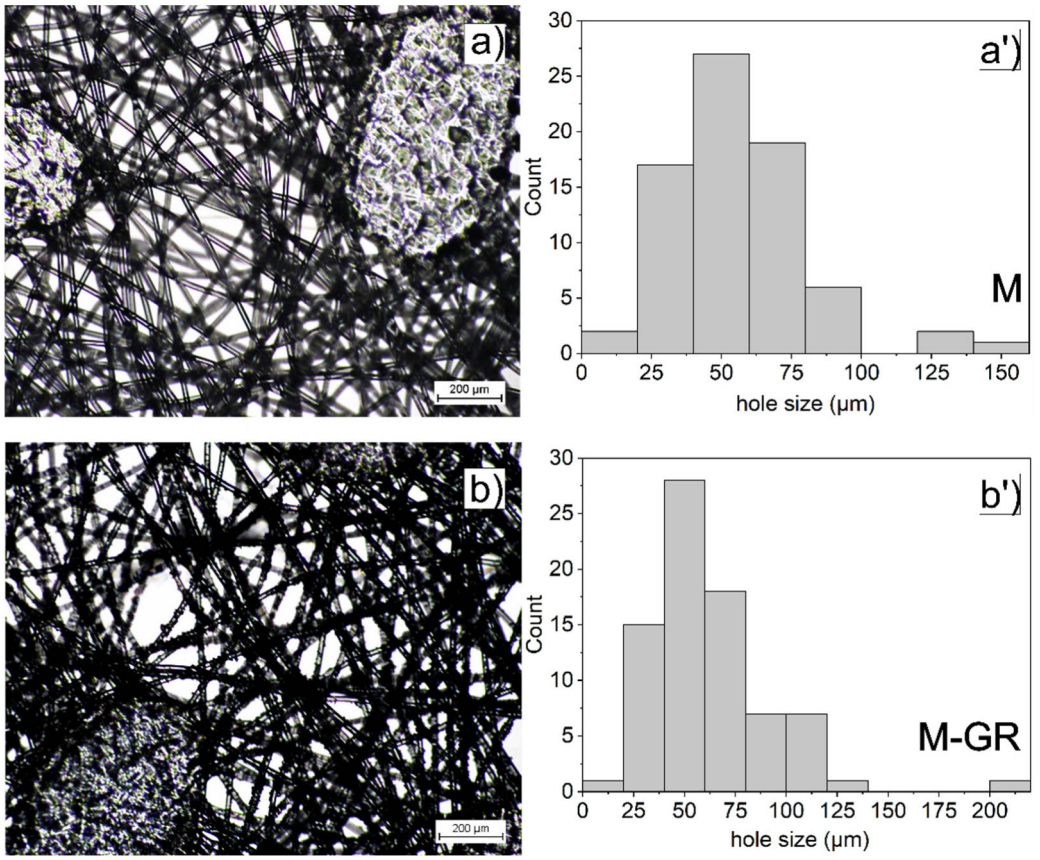

Fig. 5. Optical transmission microscopy images corresponding to the outer layer of surgical face mask (20X) (a) without and (b) with gum rosin microspheres and their respective sizes distribution of the gap between the fibres.

A comparison of the water contact angle (WCA) evolution with wearing time between the surgical face mask with and without gum rosin microspheres coating along with the sessile drop image is presented in Fig. 7. It is observed that

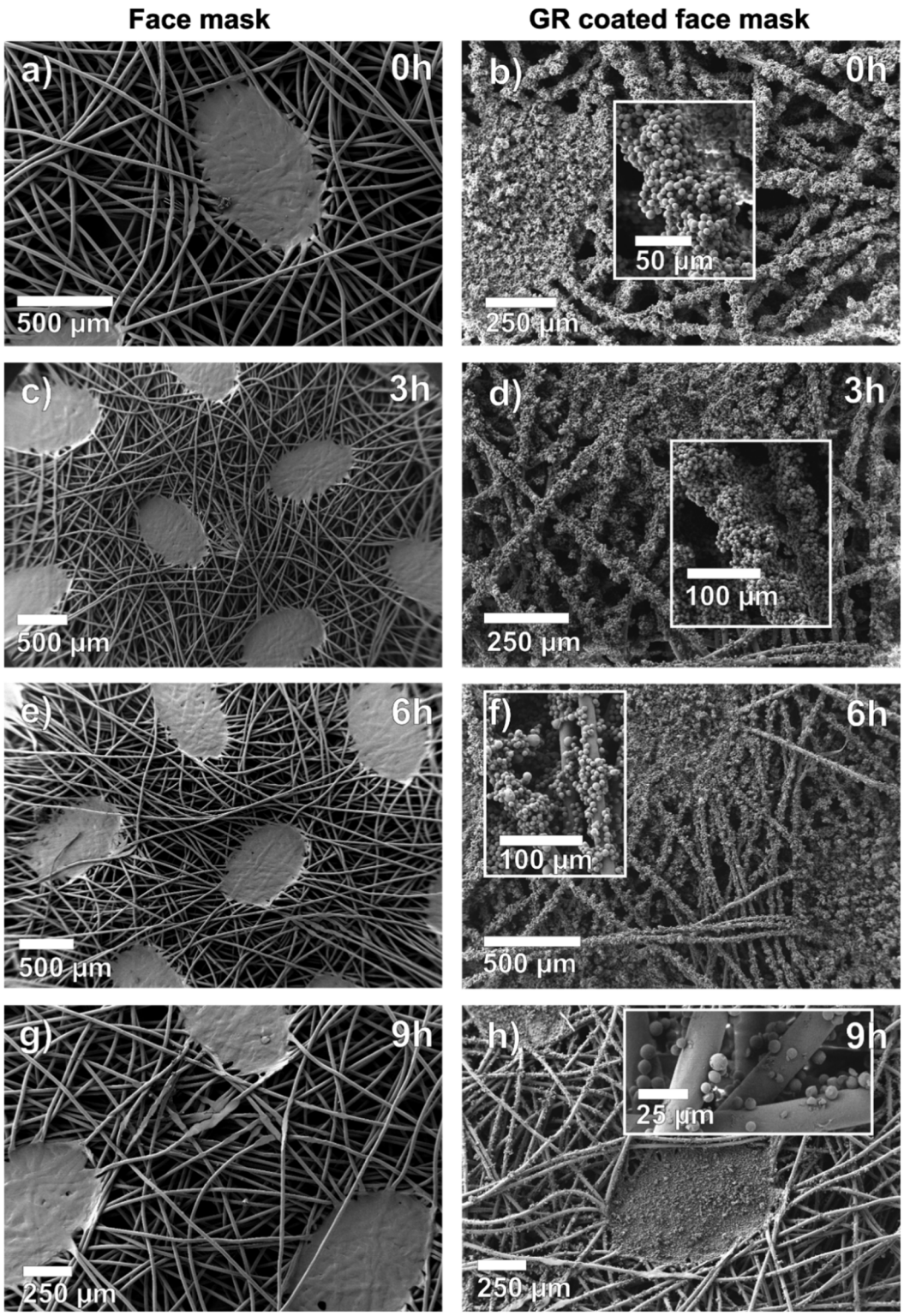

Fig. 6. Microstructure of surgical face mask without gum rosin microspheres coating at (a) 0 h, (c) 3 h, (e) 6 h and (g) 9 h of use, and microstructure of surgical face mask with gum rosin microspheres coating at (b) 0 h, (d) 3 h, (f) 6 h and (h) 9 h of wearing.

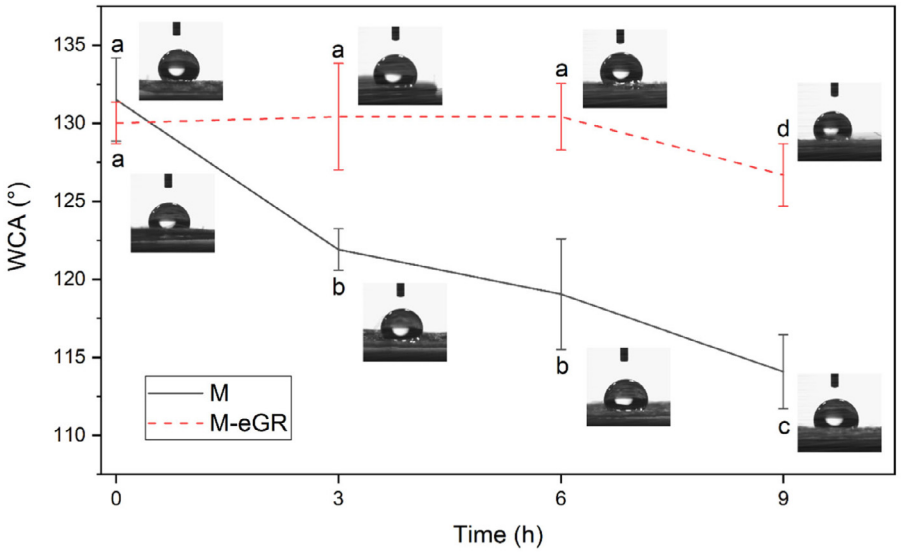

Fig. 7. Evolution of surgical face mask surface water contact angle (WCA) with and without gum rosin microspheres coating as a function of wearing time. $^{a-d}$ Different letters show statistically significant differences between formulations ($p < 0.05$).

the surface of surgical face mask with and without the microspheres coating is hydrophobic (WCA > 65°) for all the studied times (Hambleton et al., 2009; Vogler, 1998). Before wearing the mask (time = 0 h), it is seen that there are no statistical differences between the WCA of the free surface of the surgical face mask and the WCA of the surface coated with gum rosin microspheres, with a mean WCA value of 131 ± 3°. In the face mask sample (M), the WCA is reduced with the wearing time of the mask, and the differences with the 0 h are statistically significant confirming the well-known reduction efficiency of face masks during wearing. In gum rosin coated face mask (M-eGR), no significant differences with the mask before wearing (at time 0 h) were detected in the WCA until 6 wearing hours. This result is in good agreement with the FESEM images, which show that the beginning of the detachment of gum rosin microspheres takes place from hour 6. At 9 wearing hours, a significant decrease in the WCA of M-eGR was observed (127 ± 2°). However, even with this decrease, the WCA of M-eGR is higher than the WCA of M sample after 3 wearing hours. The increase in hydrophobicity in the M-eGR mask can be a consequence of a combined effect of both the hydrophobicity nature of GR (Pavon et al., 2020a) and the increased roughness produced by the bulge of GR microspheres on the surface of the fibres (Liang et al., 2018).

The WCA analyses reveal that the GR microspheres coating did not affect the initial WCA of the surgical face mask. However, the PP fibres of face mask during the contact with water show higher structural changes with higher times (9 h), as it was showed in optical microscopic images (Fig. 6g), in which the surface become more hydrophilic as the contact angle decrease. Meanwhile, in the case of coated face mask the microspheres have adhered to the polypropylene fibres obstructing the interaction between water and PP-fibres and, thus, they improved the hydrophobic behaviour during the face mask-wearing time by delaying the direct contact of PP non-woven fibres with water, which helps to maintain the protective effect of the surgical face mask for a longer time (Li et al., 2006a). Moreover, the intrinsic gum rosin tackifying effect could help to block the entrance of droplets from the outside and delay the contact of droplets with the face mask, while the antimicrobial effect could help to prevent contamination in the mask surface.

It is worth mentioning that this study is the basis for future studies where the microspheres can be used as carriers of active compounds to provide specific characteristics to the coated materials. As well, gum rosin microspheres can help to prevent the entry of viruses and bacteria and reduce the risk of spread which will allow the control of COVID-19 and other diseases.

4. Conclusions

The polypropylene outer layer of surgical face masks was successfully coated with gum rosin microspheres through the electrospraying technique. The correct deposition of the microspheres over the face mask was confirmed by thermal analyses and Fourier transform infrared spectroscopy (FTIR). The differential scanning calorimetry (DSC) analysis showed that the addition of GR microspheres coating did not affect the glass transition temperature of PP. The FTIR analysis showed that the layer of GR microspheres was present in the face mask outer layer. It was determined that GR microspheres coating has a synergistic effect with the polypropylene fibres, which increase the maximum degradation rate temperature of the face mask as was demonstrated by TGA. The FESEM images revealed that the GR microspheres have well adhered

to the polypropylene nonwoven fibres until 6 wearing hours, and the wettability analyses showed that until this time, the WCA did not decrease with the wearing time of the mask. These results show that gum rosin microspheres successfully maintain the hydrophobicity behaviour of face masks during 6 h preventing external moisture from entering the mask material better than an uncoated face mask. As well, the addition of a GR microspheres coating could help to extend the wearing time of surgical face masks and, thus, extending their service life. It should be highlighted that extending the service life of surgical masks will not only improve the face masks' efficiency but also will reduce their negative impact on the environment as less amount of them will be consumed.

The authors warn that the reported method to enhance the hydrophobicity of surgical face mask is in an experimental stage and more analyses are needed until this method is deemed safe by the correct governing bodies. Nevertheless, it should be highlighted that it can be a starting point to increase the service life of face masks by a simple and scalable method already available at industrial level.

CRediT authorship contribution statement

Cristina Pavon: Investigation, Data curation, Formal analysis, Writing – original draft. **Miguel Aldas:** Formal analysis, Methodology, Writing – review & editing. **Emilio Rayón:** Investigation, Methodology, Visualization. **Marina Patricia Arrieta:** Validation, Supervision, Writing – review & editing. **Juan López-Martínez:** Conceptualization, Funding acquisition, Project administration, Resources.

Declaration of competing interest

The authors declare that they have no known competing financial interests or personal relationships that could have appeared to influence the work reported in this paper.

Acknowledgements

This research was funded by the Spanish Ministry of Economy and Competitiveness (MINECO), project: PROMADEPCOL (MAT2017-84909-C2-2-R). Cristina Pavon thanks Santiago Grisolía fellowship (GRISOLIAP/2019/113) from Generalitat Valenciana. Miguel Aldas thanks Secretaria de Educación Superior, Ciencia, Tecnología e Innovación (SENESCYT, Ecuador) and Escuela Politécnica Nacional.

References

Abdi, M., 2020. Coronavirus disease 2019 (COVID-19) outbreak in Iran: Actions and problems. Infect. Control Hosp. Epidemiol 41, 754–755. http://dx.doi.org/10.1017/ice.2020.86.

Aldas, M., Ferri, J.M., Lopez-Martinez, J., Samper, M.D., Arrieta, M.P., 2020. Effect of pine resin derivatives on the structural, thermal, and mechanical properties of Mater-Bi type bioplastic. J. Appl. Polym. Sci. 137, 48236. http://dx.doi.org/10.1002/app.48236.

Alehosseini, A., Ghorani, B., Sarabi-Jamab, M., Tucker, N., 2018. Principles of electrospraying: A new approach in protection of bioactive compounds in foods. Crit. Rev. Food Sci. Nutr 58, 2346–2363. http://dx.doi.org/10.1080/10408398.2017.1323723.

Anu Bhushani, J., Anandharamakrishnan, C., 2014. Electrospinning and electrospraying techniques: Potential food based applications. Trends Food Sci. Technol 38, 21–33. http://dx.doi.org/10.1016/j.tifs.2014.03.004.

Armentano, I., Barbanera, M., Carota, E., Crognale, S., Marconi, M., Rossi, S., Rubino, G., Scungio, M., Taborri, J., Calabrò, G., 2021. Polymer materials for respiratory protection: Processing, end use, and testing methods. ACS Appl. Polym. Mater. 3, 531–548. http://dx.doi.org/10.1021/acsapm.0c01151.

Arrieta, M.P., García, A.D., López, D., Fiori, S., Peponi, L., 2019. Antioxidant bilayers based on PHBV and plasticized electrospun PLA-PHB fibers encapsulating catechin. Nanomaterials 9, 1–14. http://dx.doi.org/10.3390/nano9030346.

Arrieta, M.P., Perdiguero, M., Fiori, S., Kenny, J.M., Peponi, L., 2020. Biodegradable electrospun PLA-PHB fibers plasticized with oligomeric lactic acid. Polym. Degrad. Stab 179, 109226. http://dx.doi.org/10.1016/j.polymdegradstab.2020.109226.

Azémard, C., Vieillescazes, C., Ménager, M., 2014. Effect of photodegradation on the identification of natural varnishes by FT-IR spectroscopy. Microchem. J 112, 137–149. http://dx.doi.org/10.1016/j.microc.2013.09.020.

Baek, W.Il, Nirmala, R., Barakat, N.A.M., El-Newehy, M.H., Al-Deyab, S.S., Kim, H.Y., 2011. Electrospun cross linked rosin fibers. Appl. Surf. Sci 258, 1385–1389. http://dx.doi.org/10.1016/j.apsusc.2011.09.082.

Cabaret, T., Boulicaud, B., Chatet, E., Charrier, B., 2018. Study of rosin softening point through thermal treatment for a better understanding of maritime pine exudation. Eur. J. Wood Wood Prod 76, 1453–1459. http://dx.doi.org/10.1007/s00107-018-1339-3.

Calhoun, A., 2016. Polypropylene. In: Multilayer Flexible Packaging, second ed. Elsevier Inc., pp. 35–45. http://dx.doi.org/10.1016/B978-0-323-37100-1.00003-X.

Correa, J.de.S., dos Santos, R.R., Anaissi, F.J., 2018. Purification and characterization of colophony extracted of Pinus elliottii (Engelm, var. elliottii). Orbital 10, 200–203. http://dx.doi.org/10.17807/orbital.v10i3.1100.

Czigány, T., Ronkay, F., 2020. Editorial corner - a personal view the coronavirus and plastics. Express Polym. Lett 14, 510–511. http://dx.doi.org/10.3144/expresspolymlett.2020.41.

El-Atab, N., Qaiser, N., Badghaish, H., Shaikh, S.F., Hussain, M.M., Hussain, M.M., 2020. Flexible nanoporous template for the design and development of reusable anti-COVID-19 hydrophobic face masks. ACS Nano 14, 7659–7665. http://dx.doi.org/10.1021/acsnano.0c03976.

Fabra, M.J., López-Rubio, A., Lagaron, J.M., 2016. Use of the electrohydrodynamic process to develop active/bioactive bilayer films for food packaging applications. Food Hydrocoll 55, 11–18. http://dx.doi.org/10.1016/j.foodhyd.2015.10.026.

Fang, J., Zhang, L., Sutton, D., Wang, X., Lin, T., 2012. Needleless melt-electrospinning of polypropylene nanofibres. J. Nanomater. http://dx.doi.org/10.1155/2012/382639.

Favvas, E.P., Kouvelos, E.P., Papageorgiou, S.K., Tsanaktsidis, C.G., Mitropoulos, A.C., 2015. Characterization of natural resin materials using water adsorption and various advanced techniques. Appl. Phys. A Mater. Sci. Process 119, 735–743. http://dx.doi.org/10.1007/s00339-015-9022-6.

Gaillard, Y., Mija, A., Burr, A., Darque-Ceretti, E., Felder, E., Sbirrazzuoli, N., 2011. Green material composites from renewable resources: Polymorphic transitions and phase diagram of beeswax/rosin resin. Thermochim. Acta 521, 90–97. http://dx.doi.org/10.1016/J.TCA.2011.04.010.
Gao, J., Huang, X., Xue, H., Tang, L., Li, R.K.Y., 2017. Facile preparation of hybrid microspheres for super-hydrophobic coating and oil-water separation. Chem. Eng. J 326, 443–453. http://dx.doi.org/10.1016/j.cej.2017.05.175.
Grebowicz, J., Wunderlich, B., Lau, S., 1984. The thermal properties of polypropylene. J. Polym. Sci. Polym. Symp 71, 19–37.
Hambleton, A., Fabra, M.J., Debeaufort, F., Dury-Brun, C., Voilley, A., 2009. Interface and aroma barrier properties of iota-carrageenan emulsion-based films used for encapsulation of active food compounds. J. Food Eng 93, 80–88. http://dx.doi.org/10.1016/j.jfoodeng.2009.01.001.
Jefferson, T., Del Mar, C., Dooley, L., Ferroni, E., Al-Ansary, L.A., Bawazeer, G.A., Van Driel, M.L., Foxlee, R., Rivetti, A., 2009. Physical interventions to interrupt or reduce the spread of respiratory viruses: Systematic review. BMJ 339 (792), http://dx.doi.org/10.1136/bmj.b3675.
Karlberg, A.-T., 2000. Colophony. In: HandBook of Occupational Dermatology. Springer Berlin Heidelberg, Berlin, Heidelberg, pp. 509–516. http://dx.doi.org/10.1007/978-3-662-07677-4_64.
Karlberg, A.T., Gäfvert, E., Lidén, C., 1995. Environmentally friendly paper may increase risk of hand eczema in rosin-sensitive persons. J. Am. Acad. Dermatol 33, 427–432. http://dx.doi.org/10.1016/0190-9622(95)91388-2.
Kavitha Sri, A., Deeksha, P., Deepika, G., Nishanthini, J., Hikku, G.S., Antinate Shilpa, S., Jeyasubramanian, K., Murugesan, R., 2020. Super-hydrophobicity: Mechanism, fabrication and its application in medical implants to prevent biomaterial associated infections. J. Ind. Eng. Chem. http://dx.doi.org/10.1016/j.jiec.2020.08.008.
Khan, M.K.I., Nazir, A., Maan, A.A., 2017. Electrospraying: a novel technique for efficient coating of foods. Food Eng. Rev 9, 112–119. http://dx.doi.org/10.1007/s12393-016-9150-6.
Krishnaswamy, V.G., 2020. A deeper perspective on face masks - a medical aid during severe acute respiratory syndrome (sars) epidemic. J. Dis. Glob. Heal 13, 13–20.
Lasprilla-Botero, J., Torres-Giner, S., Pardo-Figuerez, M., Álvarez-Láinez, M., M. Lagaron, J., 2018. Superhydrophobic bilayer coating based on annealed electrospun ultrathin poly(ε-caprolactone) fibers and electrosprayed nanostructured silica microparticles for easy emptying packaging applications. Coatings 8 (173), http://dx.doi.org/10.3390/coatings8050173.
Leung, C.C., Lam, T.H., Cheng, K.K., 2020. Mass masking in the COVID-19 epidemic: people need guidance. Lancet http://dx.doi.org/10.1016/S0140-6736(20)30520-1.
Li, Y., Leung, P., Yao, L., Song, Q.W., Newton, E., 2006a. Antimicrobial effect of surgical masks coated with nanoparticles. J. Hosp. Infect 62, 58–63. http://dx.doi.org/10.1016/j.jhin.2005.04.015.
Li, Y., Wong, T., Chung, J., Guo, Y.P.P., Hu, J.Y., Guan, Y.T.T., Yao, L., Song, Q.W.W., Newton, E., Hy, J.Y., Guan, Y.T.T., Yao, L., Song, Q.W.W., Newton, E., 2006b. In vivo protective performance of N95 respirator and surgical facemask. Am. J. Ind. Med 49, 1056–1065. http://dx.doi.org/10.1002/ajim.20395.
Liang, Y., Ju, J., Deng, N., Zhou, X., Yan, J., Kang, W., Cheng, B., 2018. Super-hydrophobic self-cleaning bead-like SiO 2 @PTFE nanofiber membranes for waterproof-breathable applications. Appl. Surf. Sci 442, 54–64. http://dx.doi.org/10.1016/j.apsusc.2018.02.126.
Mahendra, V., 2019. Rosin product review. Appl. Mech. Mater 890, 77–91. http://dx.doi.org/10.4028/www.scientific.net/AMM.890.77.
Organisation, W.H., 2021. WHO Coronavirus Disease (COVID-19) Dashboard | WHO Coronavirus Disease (COVID-19) Dashboard. Who.Int.
Parlin, A.F., Stratton, S.M., Culley, T.M., Guerra, P.A., 2020. A laboratory-based study examining the properties of silk fabric to evaluate its potential as a protective barrier for personal protective equipment and as a functional material for face coverings during the COVID-19 pandemic. PLoS One 15, 1–19. http://dx.doi.org/10.1371/journal.pone.0239531.
Pavon, C., Aldas, M., De La Rosa-Ramírez, H., Samper, M.D., Arrieta, M.P., López-Martínez, J., 2021. Bilayer films of poly(ε-caprolactone) electrosprayed with gum rosin microspheres: Processing and characterization. J Polym. Adv. Technol. http://dx.doi.org/10.1002/pat.5397, pat.5397.
Pavon, C., Aldas, M., López-Martínez, J., Ferrándiz, S., 2020b. New materials for 3D-printing based on polycaprolactone with gum rosin and beeswax as additives. Polymers (Basel) 12 (334), http://dx.doi.org/10.3390/polym12020334.
Pavon, C., Aldas, M., de la Rosa-Ramírez, H., López-Martínez, J., Arrieta, M.P., De La Rosa-Ramírez, H., López-Martínez, J., Arrieta, M.P., 2020a. Improvement of PBAT processability and mechanical performance by blending with pine resin derivatives for injection moulding rigid packaging with enhanced hydrophobicity. Polymers (Basel) 12, 2891. http://dx.doi.org/10.3390/polym12122891.
Ray, S.S., Park, Y.I., Park, H., Nam, S.E., Kim, I.C., Kwon, Y.N., 2020. Surface innovation to enhance anti-droplet and hydrophobic behavior of breathable compressed-polyurethane masks. Environ. Technol. Innov 20, 101093. http://dx.doi.org/10.1016/j.eti.2020.101093.
Samper, M.D., Bertomeu, D., Arrieta, M.P., Ferri, J.M., López-Martínez, J., Bartomeu, D., Arrieta, M.P., Ferri, J.M., López-Martínez, J., 2018. Interference of biodegradable plastics in the polypropylene recycling process. Materials (Basel) 11, 1–18. http://dx.doi.org/10.3390/ma11101886.
Santa Cruz Biotechnology Inc., 2009. Material safety data sheet -chemical product and company identification product name statement of hazardous nature. Gum Rosin sc-215118.
Satturwar, P.M., Fulzele, S.V., Dorle, A.K., 2003. Biodegradation and in vivo biocompatibility of rosin: A natural film-forming polymer. AAPS PharmSciTech 4, http://dx.doi.org/10.1208/pt040455.
Sharma, L., Singh, C., 2018. Composite film developed from the blends of sesame protein isolate and gum rosin and their properties thereof. Polym. Compos 39, 1480–1487. http://dx.doi.org/10.1002/pc.24088.
Sipponen, A., Laitinen, K., 2011. Antimicrobial properties of natural coniferous rosin in the European pharmacopoeia challenge test. Apmis 119, 720–724. http://dx.doi.org/10.1111/j.1600-0463.2011.02791.x.
Su, C., Li, Y., Dai, Y., Gao, F., Tang, K., Cao, H., 2016. Fabrication of three-dimensional superhydrophobic membranes with high porosity via simultaneous electrospraying and electrospinning. Mater. Lett 170, 67–71. http://dx.doi.org/10.1016/j.matlet.2016.01.133.
Tcharkhtchi, A., Abbasnezhad, N., Zarbini Seydani, M., Zirak, N., Farzaneh, S., Shirinbayan, M., 2021. An overview of filtration efficiency through the masks: Mechanisms of the aerosols penetration. Bioact. Mater. http://dx.doi.org/10.1016/j.bioactmat.2020.08.002.
Termentzi, A., Fokialakis, N., Leandros Skaltsounis, A., 2011. Natural resins and bioactive natural products thereof as potential antimicrobial agents. Curr. Pharm. Des 17, 1267–1290. http://dx.doi.org/10.2174/138161211795703807.
Vogler, E.A., 1998. Structure and reactivity of water at biomaterial surfaces. Adv. Colloid Interface Sci 74, 69–117. http://dx.doi.org/10.1016/S0001-8686(97)00040-7.
World Health Organization, 2020a. Draft LandScape of COVID-19 CandIdate Vaccines. Who.
World Health Organization, 2020b. Coronavirus disease (COVID-19): Vaccines [WWW Document]. URL https://www.who.int/news-room/q-a-detail/coronavirus-disease-(covid-19)-vaccines?gclid=Cj0KCQiA-rj9BRCAARIsANB_4AAmb8ej54CLWZ1sOiWZxY6V5WJjce-uH9I2JSU_5WU7c8CFWHzSq4EaAhJoEALw_wcB. (Accessed 11.13.20).
Yadav, B.K., Gidwani, B., Vyas, A., 2016. Rosin: Recent advances and potential applications in novel drug delivery system. J. Bioact. Compat. Polym 31, 111–126. http://dx.doi.org/10.1177/0883911515601867.
Yao, K., Tang, C., 2013. Controlled polymerization of next-generation renewable monomers and beyond. Macromolecules 46, 1689–1712. http://dx.doi.org/10.1021/ma3019574.
Zhong, H., Zhu, Z., Lin, J., Cheung, C.F., Lu, V.L., Yan, F., Chan, C.Y., Li, G., 2020. Reusable and recyclable graphene masks with outstanding superhydrophobic and photothermal performances. ACS Nano 14, 6213–6221. http://dx.doi.org/10.1021/acsnano.0c02250.